Published in final edited form as:
Clin Neurophysiol. 2009 January ; 120(1): 140. doi:10.1016/j.clinph.2008.10.152.

Intracranial mapping of auditory perception: Event-related responses and electrocortical stimulation

A. Sinai[a], **N.E. Crone**[a], **H.M. Wied**[a], **P.J. Franaszczuk**[a], **D. Miglioretti**[b], and **D. Boatman-Reich**[a,c,*]

[a]Department of Neurology, Johns Hopkins School of Medicine, 600 North Wolfe Street, Meyer 2-147, Baltimore, MD 21287, USA

[b]Center for Health Studies, Group Health Cooperative, Seattle, WA, USA

[c]Department of Otolaryngology, Johns Hopkins School of Medicine, Baltimore, MD, USA

Abstract

Objective—We compared intracranial recordings of auditory event-related responses with electrocortical stimulation mapping (ESM) to determine their functional relationship.

Methods—Intracranial recordings and ESM were performed, using speech and tones, in adult epilepsy patients with subdural electrodes implanted over lateral left cortex. Evoked N1 responses and induced spectral power changes were obtained by trial averaging and time-frequency analysis.

Results—ESM impaired perception and comprehension of speech, not tones, at electrode sites in the posterior temporal lobe. There was high spatial concordance between ESM sites critical for speech perception and the largest spectral power (100% concordance) and N1 (83%) responses to speech. N1 responses showed good sensitivity (0.75) and specificity (0.82), but poor positive predictive value (0.32). Conversely, increased high-frequency power (>60 Hz) showed high specificity (0.98), but poorer sensitivity (0.67) and positive predictive value (0.67). Stimulus-related differences were observed in the spatial-temporal patterns of event-related responses.

Conclusions—Intracranial auditory event-related responses to speech were associated with cortical sites critical for auditory perception and comprehension of speech.

Significance—These results suggest that the distribution and magnitude of intracranial auditory event-related responses to speech reflect the functional significance of the underlying cortical regions and may be useful for pre-surgical functional mapping.

Keywords

Intracranial recording; Auditory cortex; Electrocortical stimulation; Epilepsy

1. Introduction

Multi-channel recording studies have shown that cortical auditory event-related responses are widely distributed across the cortex, occurring at multiple sites in the same individuals (Woods

*Corresponding author. Address: Department of Neurology, Johns Hopkins School of Medicine, 600 North Wolfe Street, Meyer 2-147, Baltimore, MD 21287, USA. Tel.: +1 410 955 0221; fax: +1 410 955 0751. dboatma@jhmi.edu (D. Boatman-Reich).

Conflicts of interest
The authors have no financial or other conflicts of interest.

and Wolpaw, 1982; Näätänen and Picton, 1987). Cortical event-related responses to auditory stimuli can be evoked or induced. Stimulus-evoked responses, such as the early cortical N1, are phase-locked to the stimulus and obtained by trial averaging in the time domain. Stimulus-induced responses refer to modulations in the spectral power of the EEG signal that are not strictly phase-locked to the stimulus and are derived using time-frequency analyses. Both types of auditory event-related responses are considered indices of cortical sound processing (Näätänen and Picton, 1987; Tallon-Baudry and Bertrand, 1999; Crone et al., 2001; Edwards et al., 2005). However, their functional relationships to each other and to the cortical regions that are essential for auditory perception remain poorly understood.

Although electrophysiologic methods provide adequate temporal resolution for investigating cortical sound processing, which occurs on the millisecond time-scale, the spatial resolution of scalp recordings is relatively poor due to signal attenuation and spatial distortion from intervening cranial tissues (Pfurtscheller and Cooper, 1975). Similarly, information about which cortical areas are functionally critical in individuals undergoing scalp recordings is generally lacking and must be inferred from stroke or other lesion studies. In contrast, intracranial recordings are not subject to the same limitations.

Intracranial recordings, also known as electrocorticography or ECoG, are performed routinely in patients with medically intractable seizures who have subdural electrodes implanted for seizure localization and pre-surgical functional mapping. Intracranial recordings provide better spatial resolution than scalp recordings because the electrodes are located directly on the surface of the cortex. They are also less vulnerable than scalp recordings to ocular and muscle artifacts (Sinai et al., 2005). Another advantage is that intracranial recordings can be performed in conjunction with electrocortical stimulation mapping (ESM), which is used to identify cortical areas that are functionally critical for motor, language, and sensory processing for pre-surgical planning (Lesser et al., 1987; Ojemann et al., 1989; Boatman, 2004). Previous ESM studies have identified sites critical for perception and discrimination of speech and other complex sounds in the left posterior temporal lobe, corresponding to auditory association cortex (Boatman et al., 1995; Boatman and Miglioretti, 2005). Conversely, auditory processing of simple tones is rarely disrupted by ESM.

Previous intracranial recording studies have identified task-related changes in spectral power, especially in the gamma frequency range (>30 Hz), during motor, language, and sensory tasks (Liegeois-Chauvel et al., 1994; Crone et al., 1998, 2001, 2006; Sinai et al., 2005; Miller et al., 2007). Recent intracranial studies have also identified changes in the gamma band during tasks involving attention, memory, and reading (Brovelli et al., 2005; Mainy et al., 2007, 2008; Sederberg et al., 2007). Intracranial recordings are well suited for investigating these high-frequency neural responses because they are not subject to the low-pass filtering effects encountered in scalp recordings. Induced spectral changes, especially in the high gamma frequencies (>60 Hz), have been observed during auditory tasks in previous intracranial recording studies (Crone et al., 2001; Ray et al., 2003, 2008; Edwards et al., 2005; Lachaux et al.,2007; Towle et al., 2008). A study by Edwards et al. (2005) demonstrated good spatial agreement between auditory evoked responses and high-frequency gamma responses to tones. Towle et al. (2008) recently reported good spatial agreement for auditory evoked responses and high gamma responses to tones. Although auditory evoked responses to speech were not described, they found increased gamma band responses to words at cortical sites identified as essential for receptive language processing by ESM. In a separate study, increased gamma responses to speech were identified at temporal lobe sites where ESM also impaired speech perception in the same patient (Lachaux et al., 2007). These studies suggest overlap in the distributions of intracranial auditory evoked and induced responses to simple tones and in the distributions of spectral responses to complex sounds, such as speech, and cortical sites that are critical for speech perception or comprehension. However, no studies to date have

compared directly auditory event-related responses, evoked and induced, to ESM using the same auditory stimuli.

In this study, we used within-subject, repeated measures testing to compare directly auditory event-related responses, stimulus-evoked and stimulus-induced, to ESM results from the same patients using the same speech and tone stimuli. The targeted evoked response was the auditory N1, an early and prominent cortical response to the onset of a novel sound, occurring 70– 120 ms after stimulus onset, and considered a relatively robust and reliable index of sound perception (Näätänen and Picton, 1987; Tremblay et al., 2003). Stimulus-induced spectral responses were identified using a matching pursuit time-frequency analysis method (Mallat and Zhang, 1993). We computed the sensitivity, specificity, and positive predictive value of cortical auditory evoked and induced responses to evaluate their accuracy in identifying cortical sites that are essential for auditory perception.

2. Methods

2.1. Patients

We tested six consecutive adult epilepsy patients, three males and three females ages 23–58 years (mean 35.7), undergoing extraoperative ESM for pre-surgical motor and language mapping (Table 1). All had medically intractable complex partial seizures, left hemisphere dominance for language as determined by intra-carotid amobarbital injection, and subdural implantation of electrode arrays (6 × 8, 8 × 8) over lateral left cortex. Pre-surgical volumetric MRI studies showed no co-morbid neurological disorders (e.g. neoplasm). Two patients had previous anterior frontal or anterior temporal lobe resections (≤3 cm), with seizure recurrence (Pts 3 and 6). Implanted electrodes were platinum-iridium disks, 3-mm diameter, embedded 10 mm apart in medical-grade silastic arrays (Ad-Tech, Racine, Wisconsin). Electrode locations were determined by co-registration of each patient's post-surgical CT to a pre-surgical volumetric MRI and by intraoperative photographs (Boatman et al., 2000;Boatman and Miglioretti, 2005). All patients had electrodes covering the posterior superior and middle temporal gyri for clinical language mapping; five also had coverage of the anterior temporal lobe. All patients had electrodes covering the parietal lobe; five also had coverage of the inferior frontal lobe. Individual differences in the number and location of electrodes were determined by clinical circumstances. Intracranial EEG recordings localized seizure foci to the anterior temporal lobe in five patients and the anterior frontal lobe in one patient (Pt 6).

Behavioral audiometric testing confirmed that all patients had normal hearing bilaterally (≤20 dB HL, 250–8000 Hz) and normal performance on tests of auditory processing, including speech recognition in quiet and under adverse listening conditions (e.g. background noise). There was no history of speech-language, motor, or attention disorders. One patient (Pt 5) participated in a previous ESM study (Boatman and Miglioretti, 2005). Informed written consent was obtained for all participants in compliance with The Johns Hopkins Institutional Review Board.

2.2. Stimuli and tasks

2.2.1. Stimuli—Fifteen 200-ms speech and tone stimuli were generated (10-ms rise/fall times). Five were digitized consonant–vowel syllables (/ba, da, pa, ta, ga/) produced by a male speaker (44.1 kHz, 16 bit sampling; SoundForge™, Sony Inc.). The 10 tone stimuli included six steady-state tones and four frequency-modulated (FM) tones (NCH Tone/Waveform Generator, NCH Software). Steady-state tones were sine-waves generated at 500 Hz, 1000 Hz, 1200 Hz, 1500 Hz, 2000 Hz, and 4000 Hz. For the recording studies, the tones were shortened to 50 ms. FM tones were composed of linear frequency sweeps starting at 900 Hz, 1100 Hz, 1300 Hz, or 1500 Hz, with 70-ms upward or downward transitions to a 1200-Hz target

frequency. Stimuli were normalized for loudness using averaged root-mean square values (SoundForge™, Sony Inc.).

2.2.2. Auditory discrimination task—For the ESM studies, auditory perception was measured with an established binary, forced-choice (same-different) auditory discrimination task in which stimulus pairs were presented in an AX format (A = first stimulus, X = second stimulus) for comparison (Boatman et al., 1995; Boatman and Miglioretti, 2005). Twenty-five stimulus pairs were generated with an intra-pair interval of 400 ms. Fifteen pairs contained speech syllables: 10 were different (e.g./pa-ba/), five were the same (e.g./pa-pa/). Ten pairs contained tones: five steady-state and five FM tones. Perceptual testing with 10 normal-hearing adult volunteers yielded discrimination accuracy scores ≥92%. The auditory discrimination task was administered both in sound field, through a CD speaker (Colby, TF-DVD5000) located directly in front of the patient and set to a comfortable listening level, and through insert earphones (Eartone 3A) at 70 dB nHL presentation level. Patients responded verbally with ‘same’ or ‘different.’

2.2.3. Auditory event-related recording paradigm—We used a 300-trial passive auditory discrimination (odd-ball) paradigm. Two speech (/ba, da/), two steady-state tones (1000 Hz, 1200 Hz), and two FM tones (upward: starting frequency 900 Hz; downward: starting frequency 1500 Hz) stimuli were selected. One stimulus was designed as the standard (/ba/, 1000 Hz, upward FM) and repeated for 82% of trials ($N = 246$). The other stimulus was labeled the deviant (/da/, 1200 Hz, downward FM) and presented infrequently (18% trials, $N = 54$) and pseudo-randomly, with no consecutive occurrences. For one patient (Pt 4), the deviant tone stimulus was 500 Hz. Stimuli were presented binaurally and sequentially at 1000-ms intervals (offset to onset) through insert earphones at 70 dB nHL. The timing and order of stimulus presentation were controlled using the GENTASK function of the Neuroscan STIM 2 system (Compumedics Inc., El Paso, Texas).

2.2.4. Intracranial auditory mapping—ESM and intracranial recording studies were initiated 3 –4 days after electrode implantation surgery. Antiepileptic medications had been discontinued for seizure localization. Patients were tested individually at bedside in a quiet room with measured ambient noise levels not exceeding 42 dB SPL. Before testing, otoscopic examination was performed to confirm that both external ear canals were unobstructed. Patients’ hearing, middle ear function, and auditory processing abilities were re-screened to rule out surgery-related changes. All patients demonstrated baseline auditory discrimination scores of ≥96% before testing.

Auditory ESM studies were performed over a 4–8 day period in conjunction with clinical language and motor mapping studies. ESM was performed by generating five-second trains of 300-μs square-wave pulses of alternating polarity at 50 Hz between adjacent electrode pairs using a Grass cortical stimulator (Grass-Tele-factor; Astro Med) as previously described (Lesser et al., 1987; Boatman et al., 2000). ESM of auditory discrimination was performed at current thresholds between 10 and 15 mA and in the absence of after discharges or sensory-motor effects. Stimulus pairs were blocked by type (speech, tones) and presented approximately one second after current onset, with one pair presented in each five-second current period. The current remained active for the five-second period or until patients responded. Testing was performed in conjunction with clinical mapping of language functions, including auditory comprehension that was assessed with a modified version of the Token Test (DeRenzie and Vignolo, 1962). Patients were blinded to the timing of the current onset. Stimulus pairs were presented at consecutive sites and at least one stimulus pair was identical. Patients responded verbally with ‘same’ or ‘different.’ The interval between stimulus pairs was determined by the time required for each patient’s EEG to return to baseline. Speech and tone discrimination were always tested at the same electrode sites within the perisylvian region.

Speech discrimination was also tested at an average of seven non-perisylvian sites per patient. Tone discrimination was tested at as many of the same non-perisylvian sites as possible within clinical time constraints. With the exception of patient 4, tone discrimination was tested at fewer non-perisylvian sites than speech discrimination. Tone discrimination was not tested with ESM in one patient (Pt 6).

To avoid patient fatigue and over-familiarization with the stimuli, a subset of 4–8 stimulus pairs of each type were presented in sound field with electrocortical stimulation. Errors were defined as responses that were absent or incorrect. A deficit was defined when errors occurred on two or more trials at the same electrode pair (e.g. ≥25% error rate). To confirm the presence of ESM-induced auditory discrimination deficits and for consistency with the recording studies, which were conducted using insert earphones, the full 25-pair auditory discrimination task was administered binaurally through insert earphones (70 dB nHL; Eartone 3A) at all electrode sites where ESM induced an auditory discrimination deficit.

Intracranial auditory recordings were acquired in a single session the day before the ESM studies to avoid EEG artifact. Separate recordings were made for speech and tones, and each recording lasted approximately 6 min. All six patients were tested with speech stimuli; the first four patients were tested with steady-state tones and the last two with FM tones. Before the recordings, each patient's baseline EEG was reviewed by an epileptologist (NEC) to rule out epileptiform activity, frequent spiking, or other potential sources of artifact. During the recordings, patients were instructed to ignore the auditory stimuli and to watch an animated video (DVD) without sound. For each patient, continuous EEG was amplified (5 × 1000) and recorded digitally (Stellate Systems Inc.) from all subdural electrodes using a referential montage, a 1000-Hz A/D sampling rate, and a bandwidth of 0.1 –300 Hz, as in our previous studies (Crone et al., 2001; Sinai et al., 2005). The reference electrode selected was relatively inactive and located at a corner of the electrode array, distal to the posterior temporal lobe. Markers for stimulus onset times were recorded simultaneously to three marker channels (all stimuli, standard, and deviant).

2.3. Data analysis

2.3.1. ESM data—For each patient, a binary map of ESM data (±deficit) was generated for each stimulus condition (speech, tones) and mapped on the individual 3D MRI reconstructions for comparison with event-related recording results. A positive ESM finding refers to the presence of a deficit (+deficit).

2.3.2. Intracranial recordings—The continuous EEG recordings were inspected visually to identify channels with excessive artifact or epileptiform activity, which were then excluded from analysis. The remaining channels were re-montaged to a common average reference to control for differences in distance between active electrodes and the reference (Crone et al., 2001; Sinai et al., 2005). Although spatial reformatting could potentially allow high-amplitude artifact or cortical responses at one site to contaminate the reference and appear at all other sites, such widespread artifacts or responses were not evident in our data likely because of prior rejection of artifacts from the raw EEG signal and the relatively low amplitude of the high-frequency (gamma) responses relative to other signal components as discussed previously (Sinai et al., 2005). Individual trials with excessive artifact were excluded from further analysis. Time-domain averaging and time-frequency analyses were performed in MATLAB (Mathworks Inc., Natick, Massachusetts) and using custom software developed in C++ to derive the evoked responses and induced spectral power changes, respectively. All analyses were performed blinded to patients' ESM results. The sensitivity, specificity, and positive predictive value of the evoked (N1) responses and the induced spectral changes were estimated based on the total set of electrode sites where ESM induced deficits in auditory perception.

2.3.3. Time domain averaging—For each recording channel, the EEG time series for speech and tones was averaged separately across 300 trials by stimulus type (standard, deviant) using a 100-ms pre-stimulus to 300-ms post-stimulus interval. The N1 response was defined as the largest negative deflection from baseline occurring 70– 120 ms after stimulus onset. No upper limit was imposed on the latency range for the speech N1 in light of reports that these latencies may be prolonged relative to those of simple tones (Tiitinen et al., 1999; Wunderlich and Cone-Wesson, 2001). N1 peak response latencies and amplitudes were measured on the averaged deviant waveform. The deviant-evoked N1 was selected because it was considered less susceptible to stimulus repetition effects, including reduced amplitude, than the standard-evoked N1 (Davis et al., 1966; Edwards et al., 2005; Rosburg et al., 2006; Trautner et al., 2006). N1 amplitudes were compared to the 100-ms pre-stimulus baseline using a paired *t*-test with a Bonferroni correction for multiple within-patient comparisons. N1 responses that differed significantly from baseline were mapped onto each patient's 3D MRI reconstruction. The channel with the largest N1 response for tones and speech was identified independently by two experienced raters and inter-rater agreement was measured using the kappa statistic.

2.3.4. Time-frequency analysis—To identify non-phase locked modulations in the spectral power of the intracranial EEG, we used a time-frequency matching pursuit algorithm (Mallat and Zhang, 1993; Franaszczuk et al., 1998; Ray et al., 2003). This approach is well suited for spectral analysis of non-stationary EEG changes and combines advantages of other approaches, including short-term Fourier transform and wavelet transform, with improved time-frequency resolution (Ray et al., 2003, 2008). For time-frequency decomposition, the total duration of the pre-stimulus interval was 1000 ms and the total duration of the post-stimulus onset interval was 1048 ms. The entire 2048-ms epoch was used for time-frequency decomposition with matching pursuit. To identify statistically significant changes in spectral power from baseline, we used a 400-ms portion of the pre-stimulus interval (range from −500 ms to −100 ms pre-stimulus). To calculate power changes relative to baseline and to test the significance of these changes, we used a 400-ms portion of the pre-stimulus baseline interval (range from −500 ms to −100 ms) and the first 1000 ms following stimulus onset. To avoid possible spectral edge effects, we excluded the first 500 ms of the 1000-ms pre-stimulus interval and the last 48 ms of the 1048-ms interval following stimulus onset from subsequent analyses (e.g. calculation of power changes, statistical testing). We also excluded the last 100 ms of the pre-stimulus interval to avoid contamination of the baseline by time-frequency components arising from stimulus artifacts (although no stimulus artifact was detected in the post-stimulus interval). Although we did not exclude lower frequencies (e.g. alpha, beta) from the analysis, it is possible that slower power changes in lower frequencies were not optimally detected because of the short inter-stimulus interval and potential overlap between power in the baseline and power changes associated with the previous stimulus. Therefore, our results focus largely on high-frequency (e.g. gamma) activity.

The signal was decomposed into a linear combination of Gabor functions called 'atoms' using a matching pursuit algorithm (Mallat and Zhang, 1993). The time-frequency power spectrum was computed by taking the Wigner–Ville distribution of the Gabor atoms (Mallat and Zhang, 1993). Line noise, which was represented in the decomposition by distinct Gabor atoms around 60 Hz, was excluded from the spectral power computation. The baseline power at each frequency was computed by averaging over all baseline time points. Power at each post-stimulus time-frequency point was compared to the respective baseline frequency power by paired *t*-test using natural log transformation and assuming unequal variances (Zygierewicz et al., 2005). To account for multiple within-subject comparisons that increase the likelihood of a type I error, a Bonferroni correction was applied. The time-frequency power spectra of the baseline segment and the post-stimulus activation segment were computed for each stimulus type (deviant, standard). The resulting values were plotted to show the magnitude and statistical significance of power changes over time. The time-frequency points (pixels) representing

statistically significant changes from baseline were plotted across the frequency range for each stimulus type (deviant, standard) and condition (speech, tones).

2.3.5. Statistics—Comparisons of event-related response latencies and amplitudes by stimulus type (tones, speech) were performed using paired *t*-tests. Statistically significant results were verified with a non-parametric alternative, the Wilcoxon matched pairs signed-ranks test. The sensitivity and specificity of event-related responses were estimated from the probability of a response occurring given the presence of an ESM deficit in speech perception (sensitivity) or of a response not occurring given the absence of an ESM deficit (specificity). Positive predictive values were calculated from sensitivity and specificity estimates and the overall prevalence of ESM deficits (10%). We used the kappa statistic to measure inter-rater reliability for selection of recording channels with the largest event-related responses, with $k \geq 0.81$ indicating very good agreement (Landis and Koch, 1977).

3. Results

3.1. Electrocortical stimulation mapping

ESM was performed at a total of 120 electrode pairs (sites) across the six patients, with an average of 20 sites (range 9–38) tested per patient (Table 2). ESM induced transient deficits in speech perception, as measured by decreased speech discrimination accuracy, at 12 of the 120 electrode sites tested (10%), for an average of two sites (range 1–3) per patient. Retesting of all 12 sites at 1–3 day intervals reproduced the deficits in all cases. Speech perception deficits were induced at electrode sites in the middle or posterior superior temporal gyrus (Fig. 1). At all sites where speech perception was impaired, auditory comprehension was also impaired when clinical ESM mapping was performed in the same patients. Auditory discrimination of tones was tested with ESM at 84 of the original 120 electrode sites (mean 17; range 8–36/patient) across five patients (Fig. 2). One patient did not undergo tone testing (Pt 6). Electrode sites were selected for tone testing based on their location in the perisylvian region. ESM did not impair patients' ability to discriminate steady-state tones at any of the sites tested. However, ESM did impair discrimination of FM tones in the one patient tested (Pt 5).

3.2. Auditory evoked responses

Auditory N1 responses to speech and tones were elicited from all six patients. N1 responses to speech were identified at a total of 28 of the 120 ESM electrode sites tested with an average of five N1 speech sites (range 2–7) per patient (Table 2). N1 responses were evident at 10 additional sites not tested during ESM (mean 2; range 0–4/patient). The mean N1 latency for speech was 110 ± 12 ms (range 98–128) and the mean amplitude was −52 ± 30 μV (range from −21 to −94). N1 speech responses localized predominantly to the superior temporal gyrus, as well as the parietal lobe (five patients), and anterior superior temporal gyrus (two patients). N1 speech responses were also identified at frontal lobe sites in one patient (Pt 5). The maximal N1 response to speech localized to the middle or posterior superior temporal gyrus in five patients and to the temporal-parietal junction in one patient (Pt 4). In five of six patients, the maximal N1 response to speech occurred at sites where speech perception was impaired by ESM (Fig. 1). The overall accuracy of the evoked N1 speech response for identifying ESM sites critical for speech perception was estimated in terms of its sensitivity, specificity, and positive predictive value (Table 3). The probability (sensitivity) of an N1 speech response occurring at any of the sites where speech perception was impaired by ESM was 0.75 (9/12 sites). Of the 108 sites where no auditory deficits were induced by electrocortical stimulation, 89 showed no N1 response, yielding a specificity of 0.82. However, ESM disrupted speech perception at only nine of the total 28 speech N1 sites, yielding a low positive predictive value of 0.32.

N1 responses to steady-state and FM tones were observed at 4–9 electrode sites per patient (mean 6) for a total of 35 sites across the six patients. The mean N1 tone latency was 93 ± 15 ms (range 72–116) and the mean amplitude was −50 ± 16 μV (range from −28 to −69). N1 tone responses occurred predominantly over the Sylvian fissure and parietal cortex and were also identified at frontal lobe sites in three patients. The maximal N1 response to steady-state tones occurred on or just above the Sylvian fissure and showed a phase reversal at electrode sites located below it (Fig. 2). The maximal N1 response to FM tones localized to the lateral superior temporal gyrus in the two patients tested (Pts 5 and 6). In the absence of ESM deficits for steady-state tones, it was not possible to determine the sensitivity, specificity, or positive predictive value of the N1 tones responses. One patient (Pt 5) underwent ESM testing with FM tones resulting in an FM tone discrimination deficit at the same site where the maximal N1 response was observed (Fig. 2).

The mean N1 speech latency (110 ms) was significantly longer than that of tones (93 ms) when compared using a two-sided paired *t*-test ($p = 0.013$; CI: 5.46, 28.20). This result was verified with a non-parametric alternative, the Wilcoxon matched pairs signed rank sum test, which yielded a test statistic of 1.55 that was significant ($p < 0.05$). There was no significant difference in the mean N1 amplitudes for speech versus tones ($p = 0.083$; CI: −18.33, 21.91). The largest N1 response to steady-state tones localized to a different site than the maximal N1 speech response in all patients tested. There was, however, partial overlap in the distribution of all N1 responses to speech and tones, with an average of three electrode sites per patient showing responses to both stimuli. For the two patients tested with FM tones, the largest N1 response occurred at or immediately adjacent to the site of the largest speech N1 (Pts 5 and 6).

3.3. Auditory induced spectral responses

Speech induced changes in EEG spectral power occurred at 1 –5 electrode sites in each patient for a total of 12 electrode sites across patients (mean 2). Spectral responses were evident at an additional five sites not tested by ESM (range 0–4/patient). For all patients, the largest increases in spectral power were observed at sites along the superior temporal gyrus where speech perception was impaired by ESM (Fig. 1). The mean onset for speech-related changes in spectral power was 108 ± 3 ms. The frequency distribution of increased power was broadband, extending from 40 Hz to as high as 250 Hz, which was the highest frequency sampled. The frequencies with the greatest increases in power varied across patients, but were generally greatest at 105–185 Hz, corresponding to the high gamma range (>60 Hz). Speech-induced high gamma activity was evident for all six patients. Four patients also showed low gamma activity (30–60 Hz).

For all patients, the largest increases in spectral power occurred at sites where speech perception was impaired by ESM. The probability of a significant increase in spectral power occurring at any of the 12 sites where speech perception was impaired during ESM was 0.67. Of the 108 sites that were not associated with deficits during ESM testing, only two showed spectral responses, yielding a specificity of 0.98. ESM impaired speech perception at eight of the 12 sites where spectral responses were identified, yielding a positive predictive value of 0.67. At all sites where spectral responses were identified, an N1 response was also present. For four patients, the largest spectral responses mapped to the same site as the maximal N1 response to speech.

Tones induced a significant increase in spectral power relative to baseline at a total of 14 sites across all patients (mean 2; range 1–7/patient). Spectral power changes were observed primarily at temporal lobe electrode sites. The mean onset for tone-related changes in spectral power was 106 ± 2 ms. The frequency distribution of the power changes was generally greatest between 40 and 100 Hz. Three patients showed concurrent low-frequency (<35 Hz) activation. For three patients (Pts 1, 3, and 5), the largest spectral power changes occurred at the same site

as the maximal N1 tone response (Fig. 2). For patient 5, the maximal spectral change for FM tones occurred at the same site on the superior temporal gyrus where ESM induced a deficit in FM tone discrimination. Visual examination of the time-frequency plots shows little evidence for increased spectral responses to tones for three of six patients (Pts 1, 4, and 6) despite a significant change relative to baseline (Fig. 2). This is likely due to the relatively small number of significant time-frequency points (pixels) plotted for these patients.

Spectral responses to tones were generally smaller in magnitude and in distribution across frequencies than spectral responses to speech. The location of the maximal spectral response to steady-state tones and speech differed in all patients tested. For the two patients tested with FM tones, the largest N1 response occurred at, or immediately adjacent to, the same site as the largest speech N1 (Pts 5 and 6).

3.4. Reliability measures

Repeat testing at 1–3 day intervals confirmed the presence of ESM deficits at all sites identified on initial screening, consistent with previous reports of good ESM test–retest reliability (Miglioretti and Boatman, 2003). Inter-rater reliability based on a kappa statistic of $k = 0.916$ was very good for selection of channels with the largest event-related responses for speech and tones (Landis and Koch, 1977).

4. Discussion

This study compared directly the spatial distribution and magnitude of intracranial auditory event-related responses with ESM results to determine their functional relationship. We observed high spatial concordance between positive ESM findings (e.g. speech perception deficits) and the largest increases in spectral power (100% concordance) and the largest evoked N1 response (83.3%) to speech. The overall cortical distributions of speech-evoked N1 responses and spectral power changes differed in size and location, with the latter showing high specificity and the former showing high sensitivity for detecting sites critical for speech perception. The absence of ESM deficits in tone discrimination precluded estimating the accuracy of tone-elicited event-related responses.

4.1. Evoked N1 responses

Auditory evoked N1 responses were broadly distributed over the cortex, with the largest number of responses occurring at sites on the posterior superior temporal gyrus and the inferior parietal lobe, consistent with previous intracranial auditory studies (Howard et al., 2000; Brugge et al., 2003; Edwards et al., 2005). Although all patients showed partial overlap in the distribution of N1 responses to tones and speech, spatial and temporal differences were observed. N1 responses to speech clustered in the lateral superior temporal gyrus corresponding to auditory association cortex, while N1 tone responses occurred mainly in the inferior parietal region. This finding supports the view that the lateral posterior superior temporal gyrus contributes to the N1 response to complex sounds such as speech (Steinschneider et al., 1999; Eichele et al., 2005; Ahveninen et al., 2006) and is part of a functional processing stream projecting from primary auditory cortex (Howard et al., 2000; Brugge et al., 2003). Similarly, the mean latency of the N1 response to speech was significantly longer than that of tones, as previously reported (Tiitinen et al., 1999; Wunderlich and Cone-Wesson, 2001). The largest N1 response to speech and tones also occurred at different sites in all but one patient, suggesting functional-anatomic separation of the cortical generators of the N1 response to different auditory stimuli.

For five of six patients, the largest speech N1 occurred at a site where speech perception was impaired by ESM. This suggests that the magnitude of the evoked N1 response is associated

with the functional significance of the underlying cortical sites. This relationship may have been revealed because of the proximity of the intracranial recording electrodes to the underlying cortical sources. However, because multiple temporally overlapping components contribute to the evoked responses recorded from scalp electrodes, the relationship between the magnitude of the response and the functional relevance of a single underlying cortical area may be confounded in scalp recordings. The distribution of N1 speech responses showed relatively good sensitivity (0.75) for detecting sites critical for speech perception and slightly higher specificity (0.82), yielding a low rate of false positives. The N1 speech response had poor positive predictive value (0.32) suggesting a low proportion of N1 speech responses associated with positive ESM results (+deficits).

ESM did not impair patients' abilities to perceive and discriminate steady-state tones. This is consistent with previous ESM studies and likely reflects cortical encoding of frequency information in primary auditory cortex located within the Sylvian fissure and therefore not affected by ESM (Boatman et al., 1995). Additional support for this view comes from the observed phase reversals of the N1 response to steady-state tones over the Sylvian fissure, consistent with previous studies localizing the neural generators of the tone N1 to the supratemporal plane (Celesia, 1976; Näätänen and Picton, 1987; Godey et al., 2001). The sparing of tone discrimination at sites where speech sound discrimination was impaired during ESM further suggests that an impairment of auditory verbal memory cannot entirely explain patients' speech perceptual difficulties since the same discrimination paradigm was used for both tones and speech.

4.2. Induced spectral responses

For all patients, significant increases from baseline spectral power were observed in response to speech. Moreover, the largest spectral power increases were always associated with sites where ESM disrupted speech perception. This suggests a strong relationship between the magnitude of the spectral response to speech and cortical sites critical for speech perception. The distribution of spectral responses was more circumscribed than that of the evoked N1 response, encompassing a total of 12 sites across patients. The smaller distribution of spectral responses, especially in the gamma range, contrasts with previous studies of auditory and visual processing and likely reflects our choice of auditory recording paradigm, which did not impose explicit attentional demands on the listener (Fries et al., 2001; Edwards et al., 2005; Ray et al., 2008). We also did not observe increased gamma band responses for speech in the superior temporal sulcus in contrast to previous intracranial and neuroimaging reports (Liebenthal et al., 2005; Lachaux et al., 2007). One possible explanation is that the sublexical (e.g. syllable) speech stimuli and simple auditory discrimination paradigms used in our study did not require the additional phonological and/or semantic processing resources associated with the superior temporal sulcus (Scott and Johnsrude, 2003; Humphries et al., 2005; Liebenthal et al., 2005; Lachaux et al., 2007).

Spectral responses to speech were consistently broadband (40–250 Hz) with the greatest power changes occurring around 100 Hz, in the high-frequency gamma range, consistent with other intracranial studies (Edwards et al., 2005; Towle et al., 2008). No consistent patterns emerged in the onset, duration, or presence of lower frequency spectral responses to speech. Spectral responses to speech showed high specificity for identifying sites where speech perception was impaired during ESM.

Spectral responses to tones were not elicited as reliably or strongly as those for speech, with only three of six patients showing clearly visible responses in the time-frequency plots. The location of the largest spectral responses to speech and tones differed when steady-state tones were used (Pts 1–4), but were the same for FM tones (Pts 5 and 6). However, without positive

ESM findings for tones, it is not possible to determine directly the functional significance of these differences.

4.3. Stimulus effects

ESM results showed clear stimulus-related differences: perception of speech but not tones was impaired in all six patients tested. Stimulus-related differences were also evident for evoked and induced responses to speech and tones. The N1 latency for speech was consistently longer than that of tones, although there were no observable differences in amplitudes. Conversely, spectral power changes in response to speech were greater than for tones, but did not differ noticeably in onset time. These findings suggest that both evoked and induced event-related responses are sensitive to stimulus differences, but manifest them differently. As noted above, the N1 response to speech and steady-state tones occurred at different sites in all patients tested. However, the N1 response to speech and FM tones occurred at the same sites in the superior temporal gyrus. This is consistent with recent ESM findings and may reflect greater similarity of FM tones to the consonant–vowel syllables, both of which contain frequency transitions, as compared to steady-state tones (Boatman and Miglioretti, 2005).

4.4. Potential limitations

Although this study focused on within-patient comparisons, the relatively small number of patients imposes a potential limitation on the generalizability of our results. Similarly, although stimulus-related differences were observed, more systematic investigation of stimulus effects is needed to verify these findings.

4.5. Implications for pre-surgical mapping

Our results suggest that intracranial recording of auditory event-related responses to speech may be useful for pre-surgical functional mapping. For all patients, there was spatial concordance between the largest event-related responses to speech and cortical sites identified by ESM as critical for speech perception. The presence of auditory comprehension deficits at the same sites is consistent with previous ESM studies and underscores the potential utility of using intracranial auditory recordings for pre-surgical language mapping (Boatman et al., 1995; Crone et al., 2001; Miglioretti and Boatman, 2003; Sinai et al., 2005; Towle et al., 2008). We elicited intracranial recordings with a passive auditory discrimination paradigm that did not require overt attention or behavioral response further underscoring the potential utility of this approach for pre-surgical functional mapping. Because we used a relatively low-level speech perception paradigm, we may have missed other cortical sites critical for auditory comprehension including lexical-semantic and syntactic processing. Therefore, eliciting intracranial recordings with more than one language task is likely to provide the most comprehensive and efficacious approach for pre-surgical language mapping.

An initially puzzling finding was that two patients showed positive ESM findings at sites where no auditory evoked or induced response was present. In both cases, the ESM deficits occurred at immediately adjacent electrode pairs. One potential explanation is that the electrical current spread from an electrode site that was not functionally critical, and therefore not associated with an event-related response, to an immediately adjacent site that was critical thereby inducing a deficit. This view is supported by recent cortico-cortical electrical stimulation studies and studies of after-discharge propagation showing effects of electrical stimulation outside of the immediate stimulation sites (Ishitobi et al., 2000; Blume et al., 2004; Matsumoto et al., 2004; Lesser et al., 2008). Alternatively, the relatively short (200 ms), single stimuli used in the recordings may have failed to elicit responses at other sites critical for speech perception that are responsive only to longer speech samples. Additional studies are needed to determine whether longer speech stimuli might improve the efficacy of intracranial recordings for pre-surgical planning.

Although evoked responses showed good sensitivity, spectral power responses showed high specificity for identifying cortical sites critical for speech perception. Combining both approaches provides comprehensive information about the essential and non-essential cortical resources that mediate auditory perception of speech. Both types of event-related response can be obtained from the same intracranial data. Because intracranial recordings sample from multiple electrodes simultaneously, this approach can be used to guide and tailor ESM, which involves sequential testing of individual electrode sites and, therefore, is more time consuming. Recent development of techniques for real-time analysis of intracranial recording data (Lachaux et al., 2007) may further increase their potential utility for pre-surgical functional mapping.

Acknowledgments

This study was supported by NIH Grants R01-DC005645 (DBR) and R01-NS40596 (NEC). We thank Ms. Jenna Los and Ms. Leila Gingis for assistance with the figures and text.

References

Ahveninen J, Jääskeläinen I, Raij T, Bonmassar G, Devore S, Hämäläinen M, et al. Task-modulated "what" and "where" pathways in human auditory cortex. Proc Natl Acad Sci USA 2006;103(39): 14608–14613. [PubMed: 16983092]

Blume W, Jones D, Pathak P. Properties of after-discharges from cortical electrical stimulation in focal epilepsies. Clin Neurophysiol 2004;115(4):982–989. [PubMed: 15003782]

Boatman D. Cortical bases of speech perception: functional lesion studies. Cognition 2004;92(1–2):47–65. [PubMed: 15037126]

Boatman D, Miglioretti D. Cortical sites critical for speech discrimination in normal and impaired listeners. J Neurosci 2005;25:5475–5480. [PubMed: 15944375]

Boatman D, Lesser R, Gordon B. Auditory speech processing in the left temporal lobe: an electrical interference study. Brain Lang 1995;51(2):269–290. [PubMed: 8564472]

Boatman D, Gordon B, Hart J, Selnes O, Miglioretti D, Lenz F. Transcortical sensory aphasia: revisited and revised. Brain 2000;123:1634–1642. [PubMed: 10908193]

Brovelli A, Lachaux J, Kahane P, Boussaoud D. High gamma frequency oscillatory activity dissociates attention from intention in the human premotor cortex. Neuroimage 2005;28(1):154–164. [PubMed: 16023374]

Brugge J, Volkov I, Garell C, Reale R, Howard M. Functional connections between auditory cortex on Heschl's gyrus and on the lateral superior temporal gyrus in humans. J Neurophysiol 2003;90:3750–3763. [PubMed: 12968011]

Celesia G. Organization of auditory cortical areas in man. Brain 1976;99(3):403–414. [PubMed: 1000279]

Crone N, Miglioretti D, Gordon B, Lesser R. Functional mapping of human sensorimotor cortex with electrocorticographic spectral analysis II. Brain 1998;121:2301–2315. [PubMed: 9874481]

Crone N, Boatman D, Gordon B, Hao L. Induced electrocorticographic gamma activity during auditory perception. Clin Neurophysiol 2001;112(4):565–581. [PubMed: 11275528]

Crone N, Sinai A, Korzeniewska A. High-frequency gamma oscillations and human brain mapping with electrocorticography. Prog Brain Res 2006;159:275–295. [PubMed: 17071238]

Davis H, Mast T, Yoshie N, Zerlin S. The slow response of the human cortex to auditory stimuli: recovery process. Electroencephalogr Clin Neurophysiol 1966;21:105–113. [PubMed: 4162003]

DeRenzie E, Vignolo L. The token test: a sensitive test to detect receptive disturbances in aphasics. Brain 1962;85:665–678. [PubMed: 14026018]

Edwards E, Soltani M, Deouell L, Berger M, Knight R. High gamma activity in response to deviant auditory stimuli recorded directly from human cortex. J Neurophysiol 2005;94:4269–4280. [PubMed: 16093343]

Eichele T, Nordby H, Rimol L, Hugdahl K. Asymmetry of evoked potential latency to speech sounds predicts the ear advantage in dichotic listening. Cogn Brain Res 2005;24(3):405–412.

Franaszczuk P, Bergey G, Durka P, Eisenberg H. Time-frequency analysis using matching pursuit algorithm applied to seizures originating from the mesial temporal lobe. Electroencephalogr Clin Neurophysiol 1998;106:513–521. [PubMed: 9741751]

Fries P, Reynolds J, Rorie A, Desimone R. Modulation of oscillatory neuronal synchronization by selective visual attention. Science 2001;291(5508):1560–1563. [PubMed: 11222864]

Godey B, Schwartz D, de Graaf J, Chauvel P, Liegeois-Chauvel C. Neuromagnetic source localization of auditory evoked fields and intracerebral evoked potentials: a comparison of data in the same patients. Clin Neurophysiol 2001;112:1850–1859. [PubMed: 11595143]

Howard M, Volkov I, Mirsky R, Garell P, Noh M, Granner M, et al. Auditory cortex on the human posterior superior temporal gyrus. J Comp Neurol 2000;416:79–92. [PubMed: 10578103]

Humphries C, Love T, Swinney D, Hickok G. Response of anterior temporal cortex to syntactic and prosodic manipulations during sentence processing. Hum Brain Mapp 2005;26(2):128–138. [PubMed: 15895428]

Ishitobi M, Nakasato N, Suzuki K, Nagamatsu K, Shamoto H, Yoshimoto T. Remote discharges in the posterior language area during basal temporal stimulation. Neuroreport 2000;11(13):2997–3000. [PubMed: 11006982]

Lachaux J, Jerbi K, Bertrand O, Minotti L, Hoffmann D, Schoendorff B, et al. A blueprint for real-time functional mapping via human intracranial recordings. PLoS One 2007;2(10):e1094. doi:10.1371/journal.pone.0001094. [PubMed: 17971857]

Landis J, Koch G. The measurement of observer agreement for categorical data. Biometrics 1977;33:159–174. [PubMed: 843571]

Lesser R, Lüders H, Klem G, Dinner D, Morris H, Hahn J, et al. Extraoperative cortical functional localization in patients with epilepsy. J Clin Neurophysiol 1987;4:27–53. [PubMed: 3108315]

Lesser R, Lee H, Webber W, Prince B, Crone N, Miglioretti D. Short-term variations in response distribution to cortical stimulation. Brain 2008;131(6):1528–1539. [PubMed: 18337272]

Liebenthal E, Binder J, Spitzer S, Possing E, Medler D. Neural substrates of phonemic perception. Cereb Cortex 2005;15(10):1621–1631. [PubMed: 15703256]

Liegeois-Chauvel C, Musolino A, Badier J, Marquis P, Chauvel P. Evoked potentials recorded from the auditory cortex in man: evaluation and topography of the middle latency components. Electrocencephalogr Clin Neurophysiol 1994;92(3):204–214.

Mainy N, Kahane P, Minotti L, Hoffmann D, Bertrand O, Lachaux J. Neural correlates of consolidation in working memory. Hum Brain Mapp 2007;28(3):183–193. [PubMed: 16767775]

Mainy N, Jung J, Baciu M, Kahane P, Schoendorff B, Minotti L, et al. Cortical dynamics of word recognition. Hum Brain Mapp 2008;29(11):1215–1230. [PubMed: 17712785]

Mallat S, Zhang Z. Matching pursuit with time-frequency dictionaries. IEEE Trans Signal Process 1993;41:3397–3415.

Matsumoto R, Nair D, LaPresto E, Najm I, Bingaman W, Shabasaki H, et al. Functional connectivity in the human language system: a cortico-cortical evoked potential study. Brain 2004;127(10):2316–2330. [PubMed: 15269116]

Miglioretti D, Boatman D. Modeling variability in the cortical representations of human complex sound perception. Exp Brain Res 2003;153:382–387. [PubMed: 14534769]

Miller K, Leuthardt E, Schalk G, Rao R, Anderson N, Moran D, et al. Spectral changes in cortical surface potentials during motor movement. J Neurosci 2007;27(9):424–2432.

Näätänen R, Picton T. The N1 wave of the human electric and magnetic response to sound: a review and an analysis of the component structure. Psychophysiology 1987;24(4):375–425. [PubMed: 3615753]

Ojemann G, Ojemann J, Lettich E, Berger M. Cortical language localization in left, dominant hemisphere: an electrical stimulation mapping investigation in 117 patients. J Neurosurg 1989;71(3):316–326. [PubMed: 2769383]

Pfurtscheller G, Cooper R. Frequency dependence of the transmission of the EEG from cortex to scalp. Electroencephalogr Clin Neurophysiol 1975;38:93–96. [PubMed: 45909]

Ray S, Jouny C, Crone N, Boatman D, Thakor N, Franaszczuk P. Human ECoG analysis during speech perception using matching pursuit: a comparison between stochastic and dyadic dictionaries. IEEE Trans Biomed Eng 2003;50:1371–1373. [PubMed: 14656066]

Ray S, Niebur E, Hsiao S, Sinai A, Crone N. High-frequency gamma activity (80–150 Hz) is increased in human cortex during selective attention. Clin Neurophysiol 2008;119(1):116–133. [PubMed: 18037343]

Rosburg T, Trautner P, Boutros N, Korzyukov O, Schaller C, Elger C, et al. Habituation of auditory evoked potentials in intracranial and extracranial recordings. Psychophysiology 2006;43:137–144. [PubMed: 16712584]

Scott S, Johnsrude I. The neuroanatomical and functional organization of speech perception. Trend Neurosci 2003;26(2):100–107. [PubMed: 12536133]

Sederberg P, Schulze-Bonhage A, Madsen J, Bromfield E, McCarthy D, Brandt A, et al. Hippocampal and neocortical gamma oscillations predict memory formation in humans. Cereb Cortex 2007;17(5): 1190–1196. [PubMed: 16831858]

Sinai A, Bowers C, Crainiceanu C, Boatman D, Gordon B, Lesser R, et al. Electrocorticographic high gamma activity versus electrical cortical stimulation mapping of naming. Brain 2005;128:1556–1570. [PubMed: 15817517]

Steinschneider M, Volkov I, Noh M, Garell P, Howard M. Temporal encoding of the voice onset time phonetic parameter by field potentials recorded directly from human auditory cortex. J Neurophysiol 1999;82(5):2346–2357. [PubMed: 10561410]

Tallon-Baudry C, Bertrand O. Oscillatory gamma activity in humans and its role in object representation. Trend Cogn Sci 1999;3:151–162.

Tiitinen H, Sivonen P, Alku P, Virtanen J, Näätänen R. Electrcomagnetic recordings reveal latency differences in speech and tone processing in humans. Cogn Brain Res 1999;8:355–363.

Towle V, Yoon H, Castelle M, Edgar J, Biassou N, Frim D, et al. EcoG gamma activity during a language task: differentiating expressive and receptive speech areas. Brain 2008;131:2013–2027. [PubMed: 18669510]

Trautner P, Rosburg T, Dietl T, Fell J, Korzyukov O, Kurthen M, et al. Sensory gating of auditory evoked and induced gamma band activity in intracranial recordings. Neuroimage 2006;32(2):790–798. [PubMed: 16809054]

Tremblay K, Friesen L, Martin B, Wright R. Test-retest reliability of cortical evoked potentials using naturally produced speech sounds. Ear Hearing 2003;24(3):225–232.

Woods C, Wolpaw J. Scalp distribution of human auditory evoked potentials. II. Evidence for overlapping sources and involvement of auditory cortex. Electroencephalogr Clin Neurophysiol 1982;54(1):25–38. [PubMed: 6177515]

Wunderlich J, Cone-Wesson B. Effects of stimulus frequency and complexity on the mismatch negativity and other components of the cortical auditory-evoked potential. J Acoust Soc Am 2001;109:1526–1537. [PubMed: 11325124]

Zygierewicz J, Durka P, Klekowicz H, Franaszczuk P, Crone N. Computationally efficient approaches to calculating significant ERD/ERS changes in the time-frequency plane. J Neurosci Meth 2005;145:267–276.

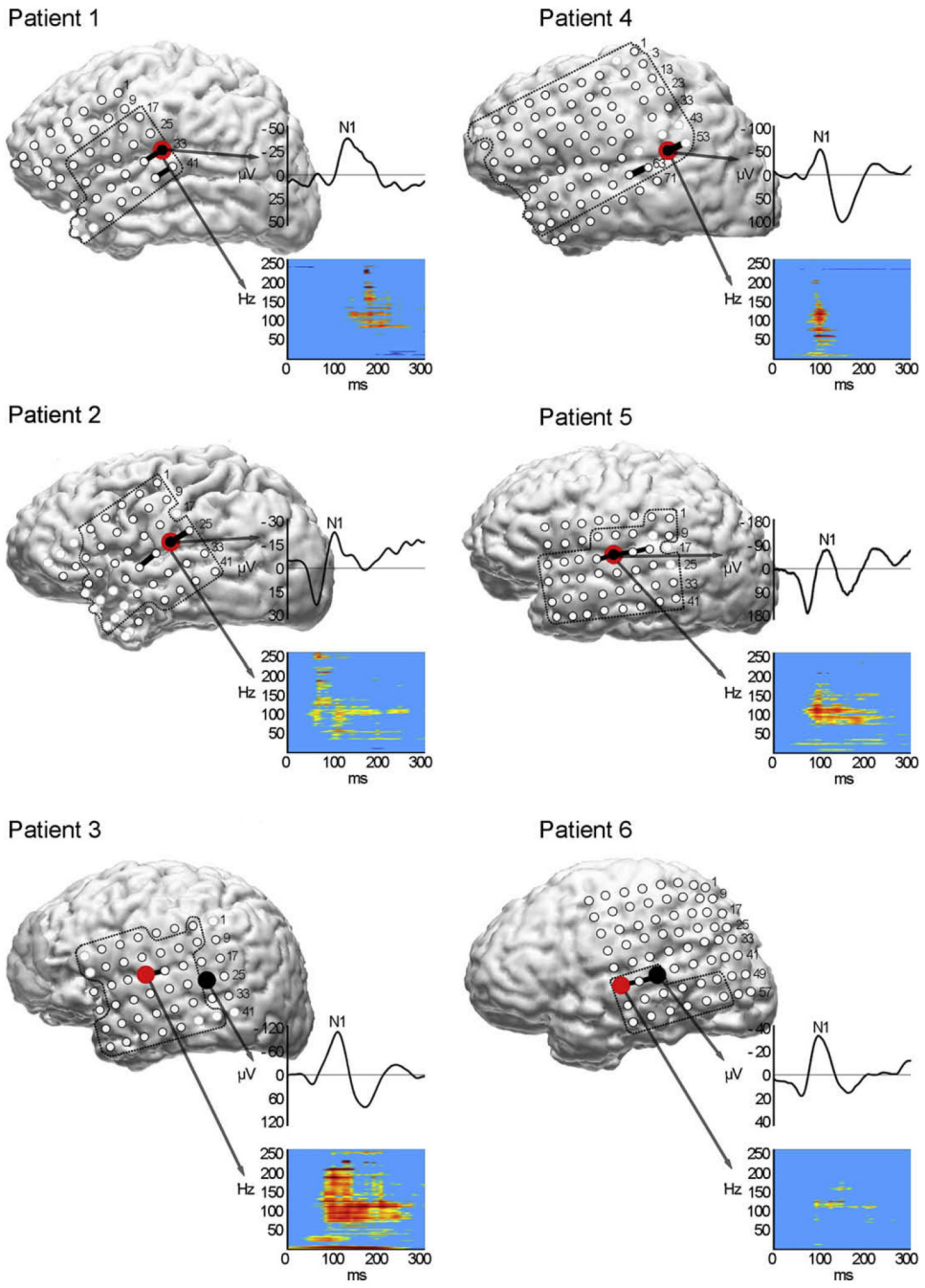

Fig. 1.

Locations of maximal evoked N1 responses (black) and spectral power responses (red) for speech and sites with speech perception deficits induced by ESM (solid black lines) co-registered with each patient's volumetric MRI. ESM was performed at electrodes inside the dotted lines. Lighter electrodes represent channels omitted from analysis due to artifact. Boxes to the right of each brain display averaged N1 waveform (top) and time-frequency spectral power plot (bottom) with time on the *x*-axis (0–300 ms). In color bar to the right of spectral plots, red represents the largest power increase. (For interpretation of the references to color in this figure legend, the reader is referred to the web version of this paper.)

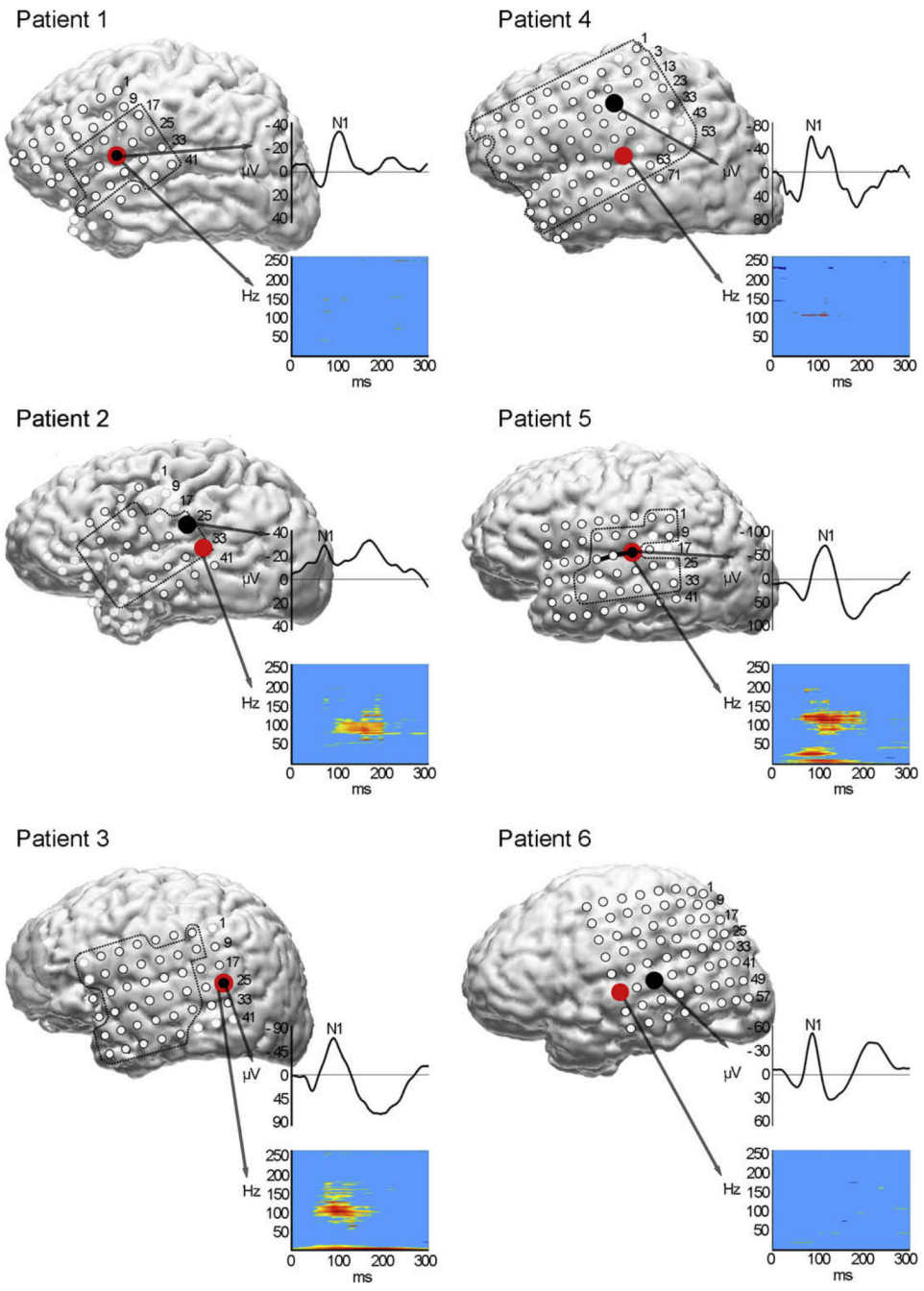

Fig. 2.

Locations of maximal evoked N1 responses (black) and spectral power responses (red) for steady-state tones (Pts 1–4) and FM tones (Pts 5 and 6) co-registered with each patient's volumetric MRI. ESM was performed at electrodes inside the dotted lines. ESM of steady-state tones was performed in patients 1–4 and with FM tones in patient 5 (+deficit: solid black line). Lighter electrodes represent channels omitted from analysis due to artifact. Boxes to the right of each brain display averaged N1 waveform (top) and time-frequency spectral power plot (bottom) with time on the *x*-axis (0–300 ms). In color bar to the right of spectral plots, red represents the largest power increase. (For interpretation of the references to color in this figure legend, the reader is referred to the web version of this paper.)

Table 1

Patient demographics.

Patient	Sex	Age (years)	Handedness	FSIQ	Seizure onset age (years)	Epilepsy duration (years)	MRI results
1	M	33	Right	94	31	2	Normal
2	F	26	Right	109	14	12	Normal
3	F	40	Right	102	20	20	Prior resection
4	M	58	Right	104	30	28	Normal
5	M	23	Left	99	4	19	Normal
6	F	34	Right	89	2	31	Prior resection
Mean		35.7		99.5	16.8	18.7	
SD		12.5		7.2	12.5	10.7	

Table 2

Summary of ESM deficits, N1 responses, and spectral power changes for auditory speech perception.

Patient	Total ESM sites tested	ESM deficit sites	N1 sites	N1 sites with ESM deficits	Spectral response sites	Spectral sites with ESM deficits
1	14	2	2	1	1	1
2	20	2	3	2	1	1
3	23	1	7	1	5	1
4	38	2	7	1	1	1
5	16	3	5	2	3	3
6	9	2	4	2	1	1
Total	120	12	28	9	12	8

Table 3

Accuracy of event-related responses for identifying sites critical for auditory perception of speech.

	Evoked N1 response	Induced spectral power response
Sensitivity	0.75	0.67
Specificity	0.82	0.98
Positive predictive value	0.32	0.67